

RSC Advances



This is an *Accepted Manuscript*, which has been through the Royal Society of Chemistry peer review process and has been accepted for publication.

Accepted Manuscripts are published online shortly after acceptance, before technical editing, formatting and proof reading. Using this free service, authors can make their results available to the community, in citable form, before we publish the edited article. This *Accepted Manuscript* will be replaced by the edited, formatted and paginated article as soon as this is available.

You can find more information about *Accepted Manuscripts* in the [Information for Authors](#).

Please note that technical editing may introduce minor changes to the text and/or graphics, which may alter content. The journal's standard [Terms & Conditions](#) and the [Ethical guidelines](#) still apply. In no event shall the Royal Society of Chemistry be held responsible for any errors or omissions in this *Accepted Manuscript* or any consequences arising from the use of any information it contains.

Cite this: DOI: 10.1039/c0xx00000x

www.rsc.org/xxxxxx

ARTICLE TYPE

Solvothermal synthesis of mesoporous manganese oxide with enhanced catalytic activity for veratryl alcohol oxidation

Ajay Jha, Tejansh Chandole, Rajan Pandya and Chandrashekhar V. Rode*

Received (in XXX, XXX) Xth XXXXXXXXXX 20XX, Accepted Xth XXXXXXXXXX 20XX

DOI: 10.1039/b000000x

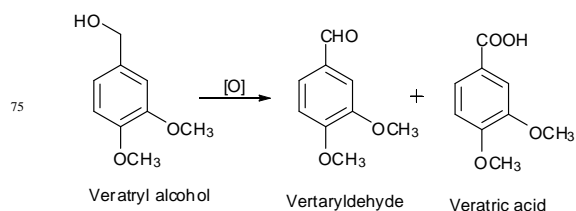
Catalyst activities of manganese and cobalt oxides prepared by solvothermal and co-precipitation methods were studied for veratryl alcohol oxidation. Manganese oxides showed higher activity performance than that of the cobalt oxides irrespective of the method of preparation. Solvothermal method yielded mesoporous manganese oxide without using any template giving mixed phases of monoclinic Mn_3O_8 and hausmannite Mn_3O_4 . The mesoporous manganese oxide exhibited excellent activity for liquid phase aerobic oxidation of veratryl alcohol under base free conditions, with 96% conversion and almost complete selectivity to veratraldehyde. The detailed characterization results on morphology, size and composition of the prepared mesoporous manganese oxide obtained by XRD, XPS, H_2 -TPR, N_2 adsorption-desorption isotherm, FE-SEM and HR-TEM technique were used to understand the role of morphological and structural features in enhancement of the observed catalytic activity.

Introduction

Activity of the catalyst strongly depends upon its morphology, crystallite size and the crystal planes hosting the active sites. These in turn depend upon the catalyst preparation methods.^{1, 2} During the past decade, rapid development in the material science offers an opportunity to prepare metal and/or metal oxides with tailored structural characteristics for efficient catalysis. Among these, the most critical factor is the exposure of a specific crystal plane which is responsible for the type of active sites required in a particular reaction.³ Our earlier studies on Co_3O_4 material synthesized by solvothermal method showed that [111] plane of the cobalt oxide was highly active, due to presence of higher concentration of Co^{3+} , responsible for the oxidation reaction.⁴ From this perspective, it was thought appropriate to compare two methods viz. co-precipitation and solvothermal for the preparation of manganese and cobalt oxides as these are versatile oxidation catalysts. In this contribution, we have compared the performances of manganese and cobalt oxide catalysts for veratryl alcohol oxidation. The structural characterization studies of cobalt oxide catalyst used in this work, have been already discussed in our previous paper.⁴

Co-precipitation is a simple and well known method, reported for the synthesis of most of the metal oxides^{5, 6} whereas, solvothermal method has been reported as a powerful tool to synthesize the nanomaterial with reproducible quality and quantitative yield.⁷ The prepared catalysts were evaluated for liquid phase oxidation of veratryl alcohol (Scheme 1). Manganese oxide is mainly used for this purpose because of its non-toxic and cost-efficient nature, and also predominantly due to the wide range of stable oxidation states (+2, +3, +4, and +7) of Mn.⁸ In heterogeneous catalysis, manganese oxides are used as selective catalysts for a wide range of catalytic applications

including ozone decomposition,⁹ photocatalytic oxidation of organic pollutants,¹⁰ nitric oxide reduction,¹¹ selective oxidations of carbon monoxide,¹² volatile organic compounds and decomposition of hydrogen peroxide.¹³ Recently, spinel Co_3O_4 , prepared by simple co-precipitation method has been reported for selective oxidation of veratryl alcohol in water by using molecular oxygen. The catalyst showed the highest conversion of 85% with 96% selectivity to veratraldehyde in 7 hours.⁵ As a derivative of coniferyl alcohol (a primary monomer of lignin), veratryl alcohol bearing 3,4-dimethoxy group has been extensively studied for understanding the chemistry of lignin valorization and exploring efficient transformation routes. Oxidation of veratryl alcohol to veratraldehyde was also reported by using different catalysts such as enzymes¹⁴, noble and non-noble metal porphyrin complexes,¹⁵ cobalt(salen) complexes¹⁶ and Co-zeolitic imidazolate frameworks (Co-ZIFs).¹⁷ However, catalyst preparation in these processes becomes tedious due to longer reaction time and the reaction being mediated by a base like pyridine or NaOH. In addition, such processes also suffer from a major problem of catalyst recovery and recyclability. Hence, it is of great practical importance to develop a simplified preparation protocol for a low cost, highly active and reusable heterogeneous catalyst with the capability to form strong redox couple and give controlled oxidation products.



Scheme 1 Aerobic oxidation products of veratryl alcohol.

Results and discussion

Manganese oxides prepared by both solvothermal and co-precipitation methods exhibited higher activity and selectivity performance than the cobalt oxide catalysts hence, the structural characterization of manganese oxide is discussed here in more detail. Manganese oxides crystallize in numerous different structures with varied proportions of Mn ions (Mn^{2+} , Mn^{3+} , and Mn^{4+}). The phases of the manganese oxide synthesized by solvothermal (MnOx-ST) and co-precipitation (MnOx-CP) methods were characterized by X-ray diffraction, and the results are shown in Fig. 1. The diffraction peaks of the sample obtained by solvothermal method were due to the mixed phases of the monoclinic Mn_5O_8 (JCPDS 39-1218) and tetragonal hausmannite of Mn_3O_4 . The latter can be considered as a spinel structure of $\text{Mn}^{2+}(\text{Mn}^{3+})_2\text{O}_4$, in which Mn^{2+} and Mn^{3+} occupy the tetrahedral and octahedral sites of the spinel, respectively.¹⁸ In case of solvothermal method, the octahedral Mn^{3+} ions in Mn_3O_4 might be oxidized to Mn^{4+} preferentially over Mn^{2+} , which could lead to the formation of $(\text{Mn}^{2+})_2(\text{Mn}^{4+})_3\text{O}_8$, i.e. the Mn_5O_8 .¹⁹ The formation of Mn_5O_8 was further proved by X-ray photoelectron spectroscopy. However, all the diffraction peaks of the sample obtained from co-precipitation were well matched with the pure tetragonal phase of Mn_3O_4 (JCPDS 24-0743).

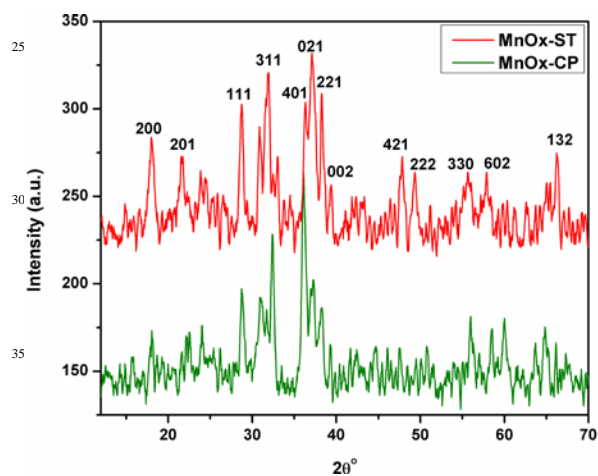


Fig. 1 XRD patterns of MnOx-ST and MnOx-CP

HR-TEM images of the manganese oxide synthesized by solvothermal (MnOx-ST) and co-precipitation (MnOx-CP) methods are shown in Fig. 2. The oxides obtained from the solvothermal method showed hexagonal nanoplate like morphology having particles size in the range of 8-12 nm whereas the oxide obtained from co-precipitation gave mixed morphology of nano-octahedron and spherical shape with the particles size in the range of 18-34 nm. The clear lattice fringe pattern illustrates that the hexagonal nanoplates are highly crystalline in nature (b) and the six side facets of the hexagonal nanoplates are well-defined. The inter-planer spacings of 0.28 nm and 0.49 nm correspond to the [311] and [200] planes of Mn_5O_8 and Mn_3O_4 , respectively. The presence of these oxide phases were also confirmed by XRD of MnOx-ST . However, inter-planer spacing of 0.27 nm obtained in case of MnOx-CP , correspond to the [103] plane of Mn_3O_4 . The field-emission scanning electron microscopy (FESEM) images in Fig.

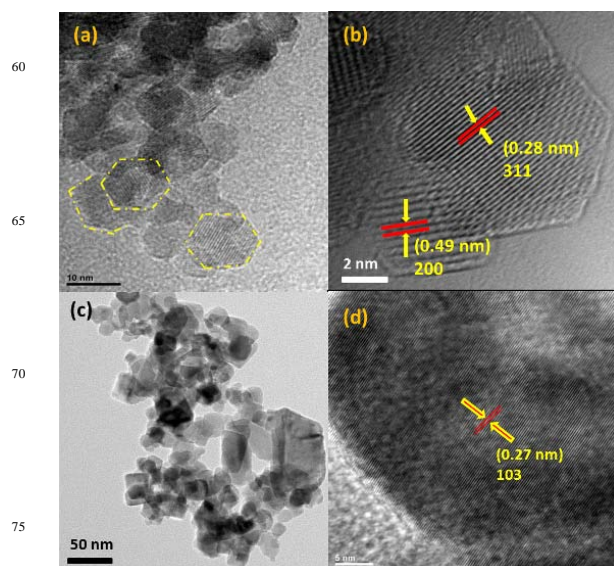


Fig. 2 HR-TEM images of (a) MnOx-ST , (b) lattice fringe pattern of MnOx-ST , (c) MnOx-CP , and (d) lattice fringe pattern of MnOx-CP .

3(a-d) show general morphology of the MnOx-ST , exhibiting several small nanosize hexagonal plates coming together to make the larger petal-like sheets with flower like appearance. The surface of the nano-hexagonal plates appeared to be highly porous.

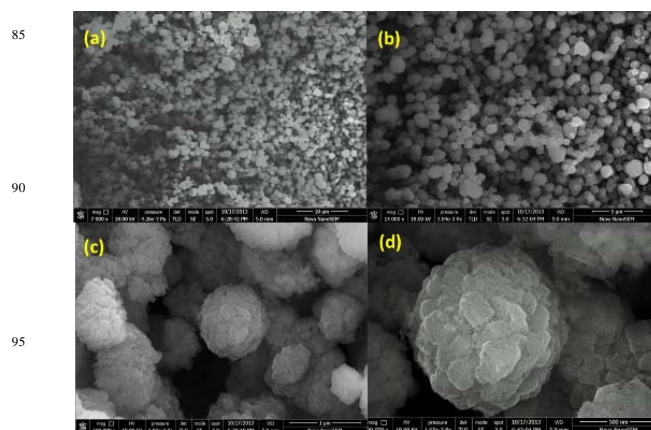


Fig. 3a-d FE-SEM images of MnOx-ST

The porous nature and specific surface area of the MnOx-ST catalyst were investigated by nitrogen adsorption measurements. Fig. 4 shows the isotherm and the corresponding Barrett–Joyner–Halenda (BJH) pore size distribution curve. The isotherm could be categorized as type IV, with a distinct hysteresis loop located in the range of 0.3–1 p/p_0 , which is a characteristic of mesoporous materials.²⁰ The hysteresis feature of the MnOx-ST at the relative pressure of 0.3-1 was classified as the H3 loop, suggesting the presence of crystalline metal oxide aggregates to form sheet like shapes.²¹ From the pore size distribution curve, it was observed that MnOx-ST catalyst showed pore size distribution with micropores in the region of 0.5-2 nm and mesopores in the range of 2 to 5 nm. The BET specific surface area of the MnOx-ST was $97 \text{ m}^2 \text{ g}^{-1}$, which was much higher than

that of MnOx-CP ($32.3\text{m}^2\text{g}^{-1}$).

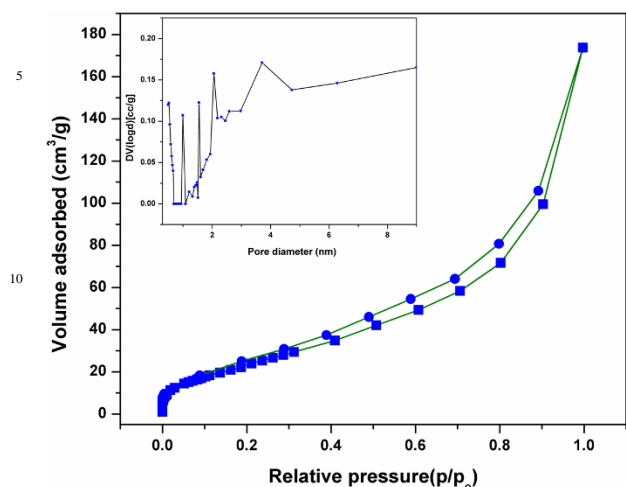


Fig. 4 N_2 adsorption-desorption isotherm for MnOx-ST and inset pore size distribution of MnOx-ST.

A typical ordered mesoporous nature of MnOx-ST catalyst was further characterized by low angle XRD result (Fig. 5), which showed a sharp diffraction peak at $2\theta = 0.9^\circ$, and could be indexed as the (211) reflection in the $Ia-3d$ space group.²² The d -value calculated from the peak was 102 \AA corresponding to the unit cell parameter, $a_0 = 25\text{ nm}$.

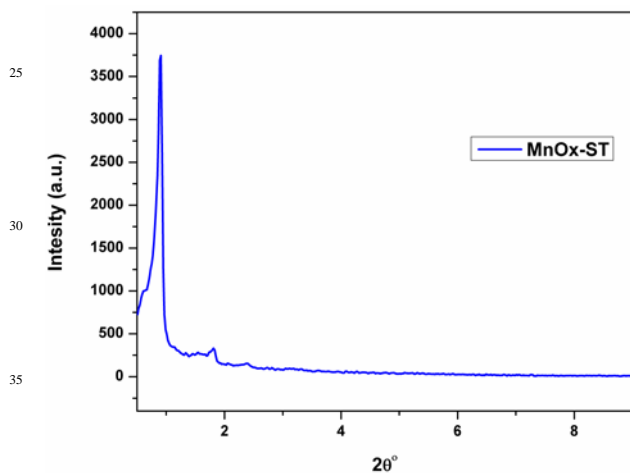


Fig. 5 Low angle XRD patterns of MnOx-ST

The H_2 -TPR profiles of MnOx-ST and MnOx-CP catalysts are shown in Fig. 6. In general, the TPR patterns strongly depended on the morphology and oxidation states of the sample. The TPR profiles of both the samples showed two step reduction processes. MnOx-CP showed the low temperature peak around $322\text{ }^\circ\text{C}$, corresponding to the reduction of Mn^{3+} ions located in octahedral holes in the hausmannite lattice. As the Mn_3O_4 particles get reduced first, relatively stable MnOx species would cover the inner core hindering further reduction, which subsequently undergo complete reduction to MnO at high temperature ($459\text{ }^\circ\text{C}$). The broad and unsymmetrical nature of the second reduction peak during reduction of MnO_x to MnO was due to the mixed morphology of MnOx-CP as also suggested by HR-TEM. However MnOx-ST, showed two very sharp and symmetrical

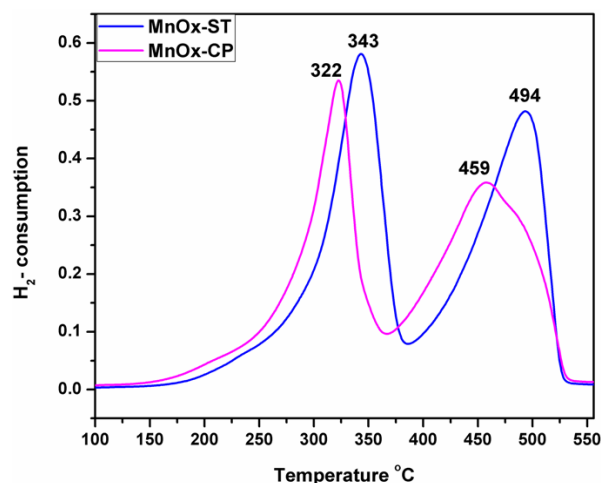


Fig. 6 H_2 -TPR profiles of MnOx-ST and MnOx-CP

reduction peaks relatively at higher temperatures ($343\text{ }^\circ\text{C}$ and $494\text{ }^\circ\text{C}$, respectively) as compared to MnOx-CP sample, indicating the uniform morphology of the MnOx-ST. The low temperature reduction peak ($343\text{ }^\circ\text{C}$) was attributed to the reduction of Mn_5O_8 to Mn_3O_4 while, the high temperature reduction peak ($494\text{ }^\circ\text{C}$) was due to the reduction of Mn_3O_4 to the MnO.²³ The H_2 consumption of MnOx-CP of 4.46 mmol/g , was close to the theoretical amount of Mn_3O_4 (4.37 mmol/g).²⁴ However in case of MnOx-ST, H_2 consumption was 6.7 mmol/g , which was much higher than the theoretical amount of Mn_3O_4 , indicating the increase of oxygen species due to the formation of Mn_5O_8 along with Mn_3O_4 .

X-ray photoelectron spectroscopy (XPS) was used to study the different oxidation states of manganese in MnOx-ST. For the MnOx-ST a broad, strong Mn $2p_{3/2}$ peak was observed suggesting Mn ion exists in more than one oxidation states. A broad signal of Mn $2p_{3/2}$ could be fitted satisfactorily to two principal peaks and two satellite peaks after deconvolution, as shown in Fig. 7A. The peaks at 641.5 and 642.7 eV correspond to Mn^{3+} and Mn^{4+} , respectively, whereas the peaks at 644 and 646.2 eV correspond to the satellite of Mn^{3+} and Mn^{4+} ions, respectively. The later were likely to be originated from the charge transfer between the outer electron shell of the ligand and the unfilled $3d$ shell of Mn during the creation of the core-hole in the photoelectron process.²⁵ Existence of two types of manganese oxides (Mn_3O_4 and Mn_5O_8) in MnOx-ST was also proved by the XRD and TPR results.

The chemical environments of oxygen in metal oxide catalysts play an important role in their catalytic properties. As shown in Fig. 7B, the O1s spectrum of MnOx-ST after deconvolution gave three peaks attributable to three types of oxygen species. The peak at BE of $529\text{--}530\text{ eV}$ was ascribed to the lattice oxygen while, the one at BE of $531\text{--}532\text{ eV}$ was ascribed to defective oxides or surface oxygen ions with low coordination. The third peak at a BE $> 533\text{ eV}$ corresponded to the adsorbed water.²⁶

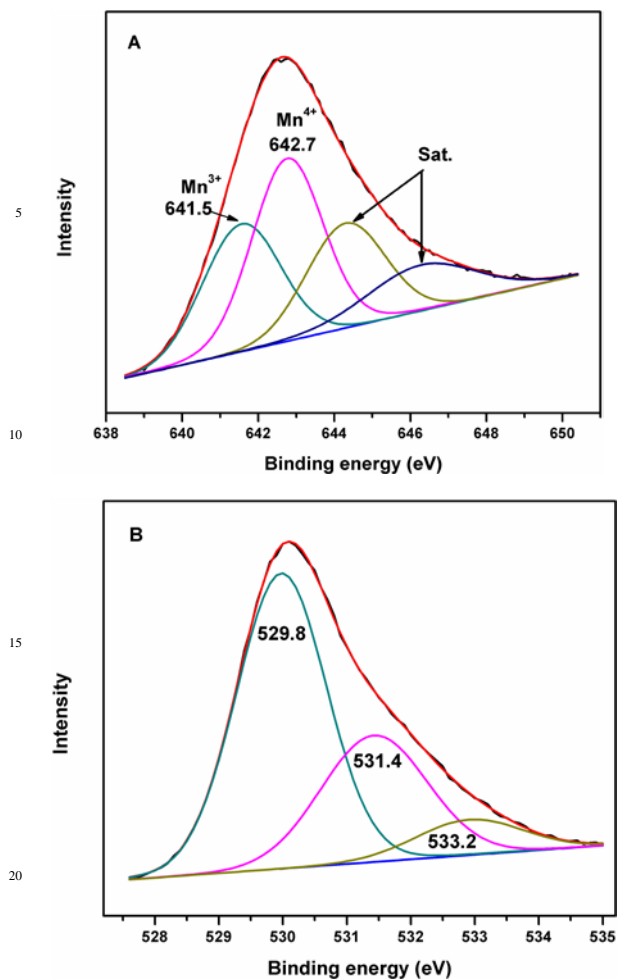


Fig. 7 XPS spectra of (A) Mn $2p_{3/2}$ and (B) O $1s$ of MnOx-ST catalyst.

Catalytic activity

The activity of manganese and cobalt oxides, prepared by solvothermal (ST) and co-precipitation (CP) methods was compared for the liquid-phase air oxidation of veratryl alcohol and the results are shown in Fig. 8. All the reactions were performed under optimum reaction conditions in the absence of a base. Among the screened catalysts, cobalt oxide based catalysts showed significantly lower conversion (CoOx-CP = 11% and CoOx-ST = 20%) than manganese oxide catalysts (MnOx-CP = 45% and MnOx-ST = 90%) with almost complete selectivity to veratraldehyde. The difference in activities could be due to the following reasons: i) Mn having higher oxygen storage capacity, ii) wide range of oxidation states, and iii) its strong reduction potential (-1.19) than that of Co (-0.27), which facilitates the oxidation process. In addition to this, the catalysts prepared by solvothermal method were found to be highly active than the catalysts prepared by co-precipitation method. The cause of higher activity of these solvothermal catalysts was due to the morphological and structural differences that enabled the exposure of more active crystal planes favourable for the oxidation reactions. As it was also confirmed from HR-TEM results; MnOx-CP showed mixed morphology of octahedron and spherical shapes with (103) plane while, MnOx-ST catalyst showed uniform regular hexagonal nanoplates with (200) and

(331) planes. The catalysts prepared by solvothermal method had higher surface area ($97 \text{ m}^2/\text{g}$) and lower particles size (8-12 nm) measured from BET and HR-TEM, respectively. This could be also the reason for higher activity of the solvothermally prepared catalyst. Highly porous nature of the material, as confirmed by FE-SEM and HRTEM, also contributed significantly to the higher activity of these catalysts. The high porosity of the material is known to enhance the diffusion rates of substrate and product and also avoids the deactivation the catalyst by pore blocking.

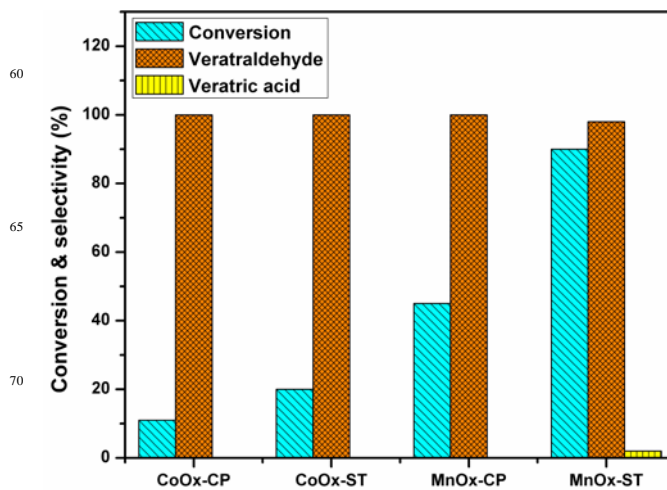


Fig. 8 Catalysts screening for veratryl alcohol oxidation. Reaction conditions: veratryl alcohol 0.5 g, catalyst (0.1 g), 120°C , acetonitrile (60 mL), air pressure (21 bar), time 90 min.

The effect of reaction time on veratryl alcohol conversion and selectivity to veratraldehyde was studied with MnOx-ST catalyst under optimised reaction conditions and the results are shown in

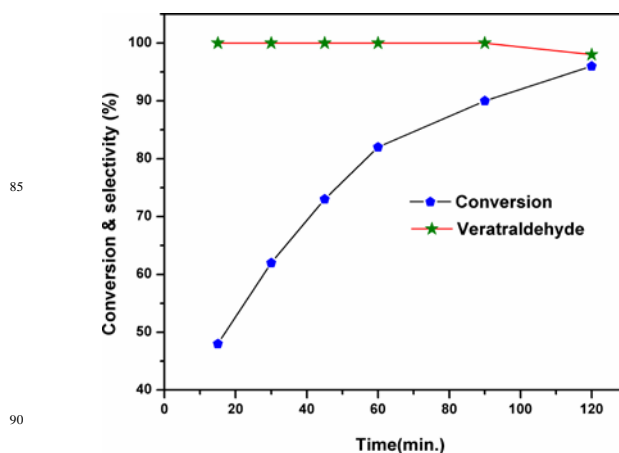


Fig. 9 Effect of reaction time on veratryl alcohol oxidation. Reaction conditions: veratryl alcohol 0.5 g, catalyst (0.1 g), 120°C , acetonitrile (60 mL), air pressure (21 bar), time 2 h.

Fig. 9. The conversion of veratryl alcohol increased from 48 to 96% with an increase in reaction time from 15 min. to 2 h. As seen from Fig. 9, the rate of conversion of veratryl alcohol, after 60 min. became slow and the selectivity to veratraldehyde started to decrease. Hence, the reaction time of 90 min. was found to be the optimum giving highest conversion and selectivity of 90%

and 98%, respectively.

The stability of the catalyst was established by its recycle experiments in the following way. After the first oxidation run with fresh MnOx-ST, the catalyst was filtered and washed several times with methanol, dried at 100 °C for 2h and reused for the subsequent runs by adding a fresh charge. Fig. 10 shows that the catalyst was found to retain its activity even after the 3rd recycle experiment with minor loss in activity (from 90% conv. to 85%) indicating the high efficiency of MnOx-ST catalyst for the oxidation of veratryl alcohol. To check the stability of the MnOx-ST catalyst and to verify that the reaction was truly heterogeneously catalyzed, a leaching experiment was also carried out. After 1h of the reaction, catalyst was filtered and the reaction was continued for another 1h, in which the conversions

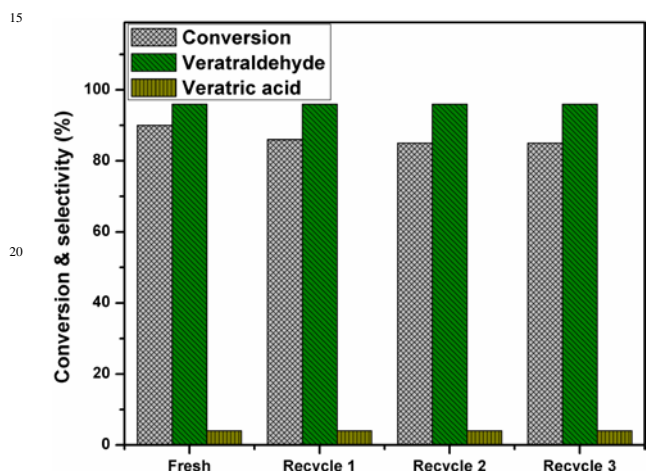


Fig. 10 MnOx-ST catalyst recycling studies. Reaction conditions: veratryl alcohol 0.5 g, catalyst (0.1 g), 120 °C, acetonitrile (60 mL), air pressure (21 bar), time 90 min.

before and after the catalyst removal were 82% and 81.5%, respectively, confirming that there was no metal leaching under the reaction conditions. Further, the used catalyst sample was also characterized by XPS (ESI Fig. S1) which confirmed that the catalyst retained its original oxidation states even after the third recycle.

Conclusions

Manganese and cobalt oxide catalysts were prepared by solvothermal and co-precipitation methods and their activities were compared for veratryl alcohol oxidation. The results showed that manganese based catalysts performed better than the cobalt oxide catalyst. It also confirmed that MnOx-ST was the best catalyst for veratryl alcohol oxidation showing 90% conversion, higher than that for MnOx-CP (49% conv.) with almost complete selectivity to veratraldehyde. HR-TEM images revealed that solvothermal method could generate the mesoporous manganese oxide with perforated hexagonal nanoplates while, co-precipitation method gave octahedron manganese oxide. FE-SEM images revealed that, MnOx-ST catalyst was highly porous and aggregate of hexagonal nanoplates exhibited flower like appearance. Activity results showed that MnOx-ST was a suitable catalyst for liquid phase veratryl alcohol oxidation carried out under base free conditions and it could be recycled three times

without any loss in activity.

Experimental section

Catalyst preparation

Mesoporous MnOx-ST catalyst was prepared by solvothermal method as described earlier.³ In a typical synthesis, 4.98 g of Mn acetate tetrahydrate was dissolved in 60 mL of ethylene glycol and the solution was gradually heated to 160 °C. To this, 200 mL of aqueous 0.2 M Na₂CO₃ solution was added drop wise and the slurry was further aged for 1 h under nitrogen atmosphere. The resulting solid was filtered, thoroughly washed with distilled water until neutralization, and dried overnight at 100 °C, then calcined at 450 °C for 4 h. CoOx-ST catalyst was also prepared by the same method. In addition Co₃O₄ and Mn₃O₄ were prepared by co-precipitation method as reported earlier.⁵

Catalytic characterization

X-ray diffractograms of the catalysts were recorded in the 2θ range of 10–80° (scan rate 5.3° min⁻¹) on a PANalytical PXRD Model XPert PRO-1712 instrument, with Ni-filtered CuKα radiation (λ = 0.154 nm) as source (current intensity, 30 mA; voltage, 40 kV) and an Xcelerator detector. Low angle powder X-ray diffractograms was collected on a Rigaku D MAX III VC diffraction system using Ni-filtered Cu Kα radiation (λ = 1.54 Å) over a 2θ range of 0.5–10° with a scan speed of 2° per minute.

Temperature-programmed reduction (TPR) experiments were performed on a Micromeritics Chemisorb 2720 instrument: the catalyst (0.05 g) was placed in a quartz tube and treated with argon gas (25 mL min⁻¹) at 200 °C for 1h. A gas mixture of 5% hydrogen in argon was then passed through the quartz reactor at 50 °C for 1 h. The temperature was raised from room temperature to 600 °C at a heating rate of 10 Kmin⁻¹ and held at 600 °C for 10 min. High-Resolution Transmission Electron Microscopy of the samples was carried out by HR-TEM, FEI Tecnai 300 and FESEM by Hitachi S-4200. X-ray photoelectron spectroscopy (XPS) analysis was performed on a VG Scientific ESCA-3000 spectrometer by using non-monochromatised MgKα radiation (1253.6 eV). To correct for possible deviations caused by electric charge of the samples, the C1s line at 284.6 eV was taken as an internal standard.

Catalytic reactions

All the catalytic oxidation reactions were carried out in a 300 mL capacity high-pressure Hastelloy reactor supplied by Parr Instruments Co. U.S.A. The reactor was connected to an air reservoir held at a pressure higher than that of the reactor. Thermo Scientific HPLC model AS3000 liquid chromatograph equipped with an ultraviolet detector was used for the liquid sample analysis. HPLC analysis was performed on a 25 cm RP-18 column. The product and reactant were detected using a UV detector at λ_{max} = 254 nm. Aqueous methanol (50%) was used as mobile phase at a column temperature of 35 °C and a flow rate of 0.7 ml/min.

In a typical experiment, 0.5 g veratryl alcohol, 0.1 g catalyst and 60 ml acetonitrile were charged into a 300 ml Parr autoclave. The reaction mixture was heated to 120 °C. After the desired temperature was attained, the reactor was pressurized with 21 bar air pressure. Then the reaction was started by agitating at 1000

rpm. The reaction was continued up to 90 min. After 90 min. the reactor was cooled to room temperature and the unabsorbed air was vented out. Then the content of the reactor was discharged and the final volume was noted down.

Acknowledgements

Authors gratefully acknowledge the Center of Excellence on Surface Science at NCL, for carrying out XPS characterization.

Notes and references

Chemical Engineering & Process Development Division, CSIR-National Chemical Laboratory, Pune-411008, Country. India Fax: +91 20 2590 2621; Tel: +91 20 2590 2349; E-mail: cv.rode@ncl.res.in

† Electronic Supplementary Information (ESI) available: [XPS of used MnOx-ST catalyst]. See DOI: 10.1039/b000000x/

- 1 H. Topsøe, *J. Catal.* 2003, **216**, 155.
- 2 A. A. Mirzaei, M. Faizi and R. Habibpour, *Appl. Catal. A: Gen.* 2006, **306**, 98.
- 3 X. Xie and W. Shen, *Nanoscale.* 2009, **1**, 50.
- 4 A. Jha and C. V. Rode, *New J. Chem.*, 2013, **37**, 2669.
- 5 V. R. Mate, M. Shirai and C. V. Rode, *Catal. Commun.*, 2013, **33**, 66.
- 6 R. B. Mane, A. M. Hengne, A. A. Ghalwadkar, S. Vijayanand, P. H. Mohite, H. S. Potdar and C.V. Rode, *Catal. Lett.*, 2010, **135**, 141.
- 7 Y. Xia, Y. J. Xiong, B. Lim and S. E. Skrabalak, *Angew. Chem. Int. Ed.*, 2009, **48**, 60.
- 8 N. N. Tušar, S. Jank and R. Gläser, *ChemCatChem*, 2011, **3**, 254.
- 9 Y. Xi, C. Reed, Y. K. Lee and S. T. Oyama, *J. Phys. Chem. B.* 2005, **109**, 17587.
- 10 H. Caot and S. L. Suib, *J. Am. Chem. Soc.*, 1994, **116**, 5334.
- 11 A. Patela, P. Shuklaa, J. Chena, T. E. Ruffordb, V. Rudolpha and Z. Zhu, *Catal. Today*, 2013, **212**, 38.
- 12 J. Xu, Y. Q. Deng, Y. Luo, W. Mao, X. J. Yang and Y. F. Han, *J. Catal.*, 2013, **300**, 225.
- 13 S. C. Kima and W. G. Shim, *Appl. Catal. B Env.*, 2010, **98**, 180.
- 14 M. Diaz-Gonzalez, T. Vidal and T. Tzanov, *Appl. Microbiol. Biotechnol.*, 2011, **89**, 1693.
- 15 C. Crestini, A. Pastoni, P. Tagliatesta, *J. Mol. Catal. A: Chem.*, 2004, **208**, 195.
- 16 J. J. Bozell, B. R. Hames and D. R. Dimmel, *J. Org. Chem.*, 1995, **60**, 2398.
- 17 J. Zakzeski, A. D. Ebczak, P. C. A. Bruijninx and B. M. Weckhuysen, *Appl. Catal., A*, 2011, **394**, 79.
- 18 Z. Tian, P. M. Kouotou, N. Bahlawane and P. H. Ngamou, *J. Phys. Chem. C*, 2013, **117**, 6218.
- 19 J. Pike, J. Hanson, L. Zhang and S. W. Chan, *Chem. Mater.*, 2007, **19**, 5609.
- 20 A. Jha, A. C. Garade, S. P. Mirajkar and C. V. Rode, *Ind. Eng. Chem. Res.*, 2012, **51**, 3916.
- 21 K. Kaneko, *J. Memb. Sci.*, 1994, **96**, 59.
- 22 F. Jiao, A. Harrison, A. H. Hill, and P. G. Bruce, *Adv. Mater.* 2007, **19**, 4063.
- 23 A. A. Mirzaei, H. R. Shaterian, M. Habibi, G. J. Hutchings and S. H. Taylor, *Appl Catal A.*, 2003, **253**, 499.
- 24 Q. F. Deng, T. Z. Ren and Z. Y. Yuan, *Reac. Kinet. Cat.*, 2013, **108**, 507.
- 25 C. C. Li, L. Mei, L. B. Chen, Q. Li and T. H. Wang, *J. Mater. Chem.*, 2012, **22**, 4982.
- 26 Y. Wua, Y. Lub, C. Songc, Z. Maa, S. Xinga, Y. Gao, *Catal. Today*, 2013, **201**, 32.

Graphical abstract

Solvothermally prepared Mn_3O_4 showed excellent performance for veratryl alcohol oxidation to veratraldehyde due to formation of monoclinic and hausmannite phases.

